

THE X-RAY CORONA OF PROCYON

J. H. M. M. SCHMITT, F. R. HARNDEN, JR., G. PERES,¹ R. ROSNER, AND S. SERIO¹

Harvard-Smithsonian Center for Astrophysics

Received 1984 April 16; accepted 1984 August 7

ABSTRACT

We have detected X-ray emission from the nearby system Procyon A/B (F5 IV + DF) using the IPC (Imaging Proportional Counter) on board the *Einstein Observatory*. Analysis of the X-ray pulse height spectrum suggests that the observed X-ray emission originates in Procyon A rather than in the white dwarf companion Procyon B, since the derived X-ray temperature, $\log T = 6.2$, agrees well with temperatures found for quiescent solar X-ray emission. Modeling Procyon's corona with loops characterized by some apex temperature T_{\max} and emission length scale L , we find that T_{\max} is well constrained, but L , and consequently the filling factor of the X-ray emitting gas, are essentially unconstrained, even when EUV emission from the transition region is included in the analysis.

Subject headings: stars: coronae — stars: individual — X-rays: sources

I. INTRODUCTION

The nearest stars are important objects of study in almost all fields of stellar astronomy because they provide observations with the highest possible spatial resolution and highest sensitivity for objects of a given class, and because the determination of their physical parameters is not plagued by distance uncertainties. One of these stars is the nearby ($d = 3.4$ pc) astrometric binary Procyon A/B. The A component of this system is a slightly evolved F star of spectral type F5 IV–V (Hoffleit 1982); its mass ($M_A = 1.77 M_\odot$; Allen 1973) is determined dynamically, its radius interferometrically (Hanbury Brown *et al.* 1967), and thus its surface gravity, one of the key parameters for determining stellar atmospheres and coronae, can be computed from directly observed quantities. The B component is a white dwarf with mass $M_B = 0.63 M_\odot$ (Allen 1973), classified as DF, and orbiting Procyon A in about 40 years; the mean apparent separation of the two stars at the present epoch is about 5".

From the X-ray point of view, Procyon A/B is a very interesting system because it contains two potential X-ray sources. However, unlike Sirius B, the X-ray emitting DA white dwarf companion of another nearby star, Procyon B is relatively cool, with surface temperatures of about 6000 K (Allen 1973). If the X-ray emission from white dwarfs is interpreted in terms of the photospheric emission model (Martin *et al.* 1982), rather than in terms of coronal emission, Procyon B is an unlikely candidate for X-ray emission. On the other hand, Procyon A was suggested as a source of coronal X-ray emission more than 10 years ago by De Loore and De Jager (1970), essentially by scaling the observed solar X-ray flux with radius and convective velocities. Subsequent attempts to detect X-ray emission from Procyon with nonimaging, soft X-ray sensitive detectors failed (Cruddace *et al.* 1975; Mewe *et al.* 1975), although the upper limits derived in these experiments already ruled out the simple scaling employed by De Loore and De Jager (1970), and the more sophisticated minimum flux corona model by Hearn (1975).

Another strong constraint on Procyon's outer atmosphere comes from ultraviolet observations of chromospheric and

transition region material. Extensive observations of Procyon were carried out with the *Copernicus*, *TD-1*, and *IUE* satellites (Evans, Jordan, and Wilson 1975; Jamar, Macon-Herbot, and Praderie 1976; Morton *et al.* 1977; Brown and Jordan 1981). The spectra obtained clearly show the presence of a chromosphere; among many other elements, the lines of Si IV, C IV, N V, and O VI were detected, indicating the presence of material temperatures of up to 3×10^5 K, i.e., at transition region temperatures. Brown and Jordan's (1981) most recent model of Procyon A utilizes all available UV observations and was consistent with the X-ray data available at the time; in their model, the emission measure drops sharply at temperatures above 3×10^5 K, and no corona is formed. Clearly, high-sensitivity X-ray observations provide the crucial link in the interpretations of the UV data with respect to the formation of chromosphere and corona, and in testing models for the outer atmospheres of cool stars such as Procyon A.

A second problem which we shall address is the interpretation of low-resolution X-ray spectra of stellar sources as obtained by the IPC (Imaging Proportional Counter) on board the *Einstein Observatory*. We shall argue below that the X-ray spectrum rules out Procyon B as a candidate for the observed X-ray source. Hence the X-ray emission must be coronal, and then the question arises which physical parameters of the underlying corona can be determined from an analysis of the IPC spectra. Procyon is prototypical in the sense that its IPC X-ray spectrum can be fitted, assuming a single-component, isothermal, optically thin plasma at a temperature below the carbon edge at 0.28 keV, i.e., at temperatures typical for quiescent solar X-ray emission. In this and subsequent papers we shall explore the constraints imposed on coronae of late-type stars from the observed IPC X-ray spectra.

II. OBSERVATIONS

Procyon was observed with the IPC on board the *Einstein Observatory* on 1981 March 31, between UT 13:47 and UT 16:54. A full description of this instrument is given by Gorenstein, Harnden, and Fabricant (1981); in this context it suffices to note that the IPC is a detector sensitive to X-rays between energies above ~ 0.15 keV (depending on the instrument gain) and below about 4.5 keV (determined by the mirror

¹ Also at Osservatorio Astronomico, Palermo, Italy.

reflectivity), with modest spectral ($\Delta E/E \sim 1$) and spatial ($\sim 1'$) resolution. In 4855.6 s of usable data, we observed 3516 counts (after background subtraction) within a radius of $3'$ centered on the X-ray source, hence yielding a count rate of 0.724 counts s^{-1} .

The observed X-ray source position is at right ascension $7^h 36^m 39^s \pm 2^s$ and declination $5^\circ 20' 38'' \pm 31''$, which agrees well with the catalog position of Procyon corrected for proper motion. On this basis alone, we are confident in identifying Procyon A/B as the source of the observed X-ray emission, but the source was also observed 1979 April 1 with the *Einstein* high-resolution imager (HRI; Giacconi *et al.* 1979), and the HRI position confirms this identification with Procyon. In fact, the HRI location $\sim 4''$ south of Procyon A (i.e., on the edge of the 90% confidence error circle of radius $\sim 4''$) indicates identification with Procyon A and not Procyon B, which was located $\sim 5''$ north of Procyon A (and hence $\sim 9''$ from the X-ray position). Furthermore, the best quality HRI data (a subset of duration ~ 320 s when the star trackers were locked onto the guide stars) shows the HRI source to be pointlike. Moreover, the low effective temperature of Procyon B as well as the detailed analysis of the IPC pulse height spectrum, which will be presented in § III, provide strong evidence that the observed X-ray emission is in fact coming from Procyon A, i.e., from a *corona* surrounding this star.

We have searched for variability of the X-ray flux on time scales larger than 200 s, but find no evidence for such variability; constancy of the observed X-ray flux over a time period of 3 hours does not contradict the interpretation of Procyon A as a coronal X-ray source.

III. ANALYSIS AND DISCUSSION

a) Emission Measure Analysis

In the course of the data processing, IPC data are subjected to a spectral analysis of the pulse height data. A first, simple model, used for stellar X-ray sources, is that of an isothermal plasma emitting a thermal line spectrum (Raymond and Smith 1977). This model then allows a determination of X-ray temperature T and volume emission measure EM ($EM = N^2 V$, where N denotes particle density and V the volume of the X-ray emitting plasma); cosmic abundances and negligible

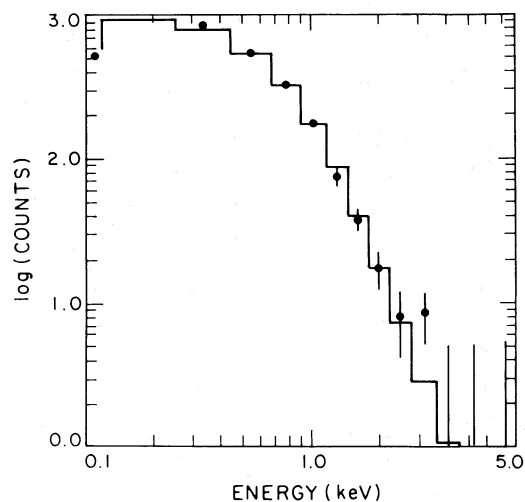


FIG. 1.—Observed and best fit predicted pulse height IPC spectrum as a function of photon energy for Procyon.

interstellar absorption are assumed. For the nominal gain at the source position, we obtain for Procyon a temperature of $\log T = 6.200^{+0.014}_{-0.021}$ and a resulting emission measure EM of $3.7 \times 10^{50} \text{ cm}^{-3}$; in Figure 1 we show the observed pulse height distribution together with the best fit model prediction.² The error distribution is asymmetric because of the broad resolution of the IPC for very soft photon energies. The 68% errors were derived by treating X-ray temperature as the single “interesting” parameter (Avni 1976). We emphasize that these errors only include *statistical* effects, and in the Appendix we demonstrate that the true error in the derived X-ray temperature is completely dominated by *systematic* effects due to uncertainties in the assumed input spectra and in the instrument calibration. Using IPC channels 1–13 for the fit, the resulting reduced χ^2 is 1.04 with 11 degrees of freedom. If we exclude the bottom channel, which has the largest (i.e., $\sim 30\%$) corrections applied to it and whose calibration may not be as well established as that of the other channels, we obtain instead a reduced χ^2 of 0.65 with 10 degrees of freedom.

The IPC pulse height spectrum provides convincing evidence that Procyon A, rather than Procyon B, is the X-ray source: IPC pulse height spectra of white dwarfs tend to be extremely soft (see Kahn *et al.* 1984), and can be fitted by simple blackbody models at temperatures of less than 100 eV. In contrast, the X-ray spectrum of Procyon cannot be adequately fitted assuming any blackbody spectrum with or without absorption at any temperature above 10 eV, whereas the thermal line spectrum provides a satisfactory fit. Procyon’s IPC pulse height spectrum (see Fig. 1) is much harder than any of the IPC pulse height spectra obtained by Kahn *et al.* (1984; see their Fig. 1) for four hot white dwarfs. Additional support for our interpretation can be derived from the HRI observations of Procyon A/B. Although the HRI is more sensitive to the EUV than the IPC, only a single point source is seen at a position consistent with Procyon A but not with Procyon B; hence, there is no evidence for X-ray emission from Procyon B, and there can be no reasonable doubt that all the X-ray emission observed in the IPC must be attributed to Procyon A, i.e., a coronal source.

Using the emission measure distribution obtained by Brown and Jordan (1981) from transition region lines only, and folding it through the IPC response at the appropriate instrument gain, we predict a count rate of ~ 5 counts ks^{-1} , more than two orders of magnitude *below* the observed count rate. The reason for this small predicted count rate is the drop in emission measure at temperatures above $\log T \sim 5.3$, derived from *Copernicus* observations of O v and O vi lines. This example clearly shows the danger of extrapolating emission measure distributions obtained from transition region lines to coronal temperatures as well as the difficulty of comparing nonsimultaneous observations in different passbands.

b) Loop Modeling

From the point of view of merely obtaining acceptable fits to the observed X-ray pulse height spectra, we are not compelled

² We wish to emphasize in this context that we do not consider the model of the X-ray emitting region just discussed, i.e., an isothermal plasma at uniform temperature, physically plausible; we shall in fact consider more realistic models in the next sections. However, assigning all the X-ray flux to plasma at a given temperature does follow the emission measure analysis performed by Brown and Jordan (1981), who assigned all the flux in a given line to plasma at a single temperature, although in reality the line emission (just as the X-ray emission) would be produced over a whole range of temperatures.

to consider models more complicated than isothermal plasmas in order to explain the observed X-ray emission from Procyon. However, the Sun's X-ray emission is coronal and is known to arise from magnetically confined plasma (loops) on all observed ranges of surface brightness down to the resolution limit (see, for example, Vaiana and Rosner 1978 and references therein). By analogy, it therefore seems reasonable to assume that Procyon's X-ray emission is also produced in similar loop structures. The question then arises whether the X-ray data allow us to determine physical parameters of the loops which we hypothesize to be present in Procyon's corona.

Since the basic ideas of loop modeling have been discussed elsewhere in great detail (see, for example, Rosner, Tucker, and Vaiana 1978; Craig, McClymont, and Underwood 1978; Golub *et al.* 1982; Giampapa *et al.* 1984; Landini *et al.* 1984), we restrict ourselves to the following remarks: Loop modeling is an energy balance analysis as compared to the emission measure analysis, carried out by Brown and Jordan (1981). Since our ultimate goal is to find a unique model, which incorporates all the physics thought to be relevant, and which is consistent with all the available observations, energy balance analysis is preferable (see Vaiana and Rosner 1978 for a detailed discussion); hence, any physical parameters we derive will only apply within the framework of the model we shall define below. The simplest nontrivial model assumes that the X-ray emission comes from static loops in hydrostatic equilibrium, i.e., the gas pressure inside a loop has to satisfy the equation

$$\frac{dp(s)}{ds} = -\frac{\mu m_H g_s p}{2k T}, \quad (1)$$

where p denotes pressure, μm_H the average ion mass, k Boltzmann's constant, T temperature, g_s the component of gravity along the loop, s a spatial coordinate along the loop, and semicircular loops with half-length L are assumed in order to fix the geometry. Further, the heat input $E_H(s)$ into the loop is locally balanced by radiative losses $E_R(s)$ and the conductive flux F_C through the energy equation

$$E_H(s) + E_R(s) = \text{div } F_C(s). \quad (2)$$

Rosner, Tucker, and Vaiana (1978) and Serio *et al.* (1981) among others have studied loop models described by equations (1) and (2) over a large parameter range and under different assumptions concerning the heating function $E_H(s)$ and flux tube cross sections; in particular, the temperature T_{max} at the loop top, the pressure p_0 at the base of the loop, and the loop length L are not independent, but related through the scaling relation (Rosner, Tucker, and Vaiana 1978), valid for large values of pressure and heating scale heights,

$$T_{\text{max}} \propto (p_0 L)^{1/3}. \quad (3)$$

In order to obtain a unique specification of a stellar loop atmosphere, a number of assumptions have to be made: We demand the X-ray emitting gas to be in hydrostatic equilibrium, which seems justified due to the absence of temporal variability of the observed X-ray radiation; further, we assume that effects arising from flux tube expansion and finite pressure and heating scale height are unimportant, i.e., that the derived coronal parameters do not sensitively depend on these parameters (see Serio *et al.* 1981; Pallavicini *et al.* 1981); last, we assume that all loops are identical and fill the available volume with some (volume) filling factor f to be determined. (Note that

$0 \leq f \leq 1$, and that for coronae whose scale height is much smaller than the stellar radius, f also corresponds to a surface filling factor; the possibility of f slightly larger than 1 is discussed below in the context of model 1.) The last assumption could be relaxed and more complicated models (involving, say, two classes of loops) considered; however, our low-resolution IPC spectra do not allow us to meaningfully constrain these models, and we will therefore only consider three parameter classes of loop models, i.e., models determined by any two of p , L and T , and f .

Because of the scaling relation (3), a loop can be specified by, say, base pressure p_0 and length L . Folding the calculated loop emission measure distribution plasma emissivities as calculated by Raymond and Smith (1977) and the IPC response function at the appropriate instrument gain, we can calculate the test statistic χ^2 , defined by

$$\chi^2 = \sum_{\text{IPC channels}} \frac{[n_i - n_{c,i}(f, L, p)]^2}{\sigma_i^2}, \quad (4)$$

where n_i , σ_i , and $n_{c,i}$ denote the observed number of counts, their uncertainty, and the predicted number of counts in the i th channel, respectively. Since the minimization with respect to f can be carried out analytically, it is sufficient to compute a grid of loop models varying p and L only, to find global minimum in χ^2 and the best fit parameters p , L , and f together with their uncertainties.

In Figure 2 we plot the contours of the test statistic χ^2 (after minimization with respect to f) versus logarithmic loop length and logarithmic base pressure; the contours shown are at $\chi^2 = 9$ through 15 in steps of 1, and the minimum values of χ^2 are ~ 7.8 . Unfortunately, in $\log(p)$ - $\log(L)$ space, the minimum value of χ^2 is not well defined, but is only known to lie along the line $\log(p) + \log(L) = \text{constant}$, in accordance with the scaling relation (3). In other words, our IPC X-ray spectra determine T , but not p and L separately. The derived filling factors for models with long, low-pressure loops become unphysically large ($f \gg 1$), and hence provide an upper bound in permissible loop length, whereas for models with short,

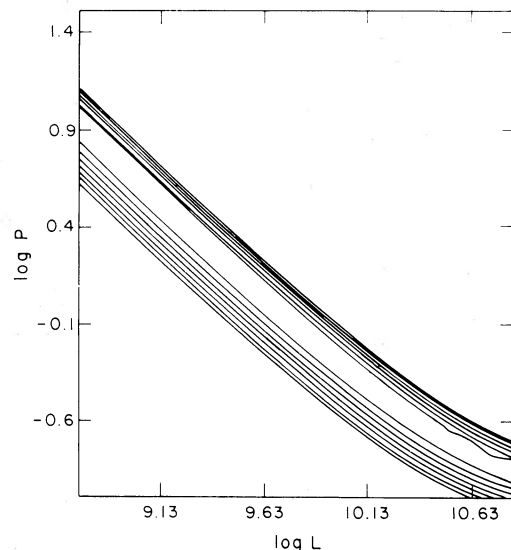


FIG. 2.—Contours of constant χ^2 as a function of $\log L$ (in cm) and $\log p$ (in dyn cm $^{-2}$); plotted contours are at $\chi^2 = 9, 10, 11, 12, 13, 14$, and 15 on either side of the minimum χ^2 valley; see text for details.

high-pressure loops, small filling factors are found ($f < 0.1$). The temperatures at the loop top are almost constant for all best fit models at values between $\log T = 6.42$, for low-pressure loops, and $\log T = 6.36$ for short, high-pressure loops. We note that these temperatures are consistently larger than those derived assuming an isothermal plasma (by up to 50%). This discrepancy is due to the combined effects of the plasma emissivity, which peaks at temperatures less than $\log T = 6.4$, and the IPC sensitivity, which drops precipitously at the carbon edge at 0.28 keV; in other words, because the radiative loss rate from coronal gas at temperatures below the temperature maximum is higher than that at the temperature maximum, and the X-ray detector is more sensitive to former emission, the derived single temperature fits result in "effective" temperatures (i.e., temperatures weighted by the emission measure distribution, plasma cooling function, and instrument response) lower than those at the loop top. Using the results of such isothermal fits as input for a loop synthesis may therefore be misleading.

Next, we consider the emission in the lines of C IV, Si IV, and N V predicted by our loop models. In contrast to the X-ray emission, which emanates from the hot, coronal portions of the loop, the EUV line emission arises predominantly from the transition region, at temperatures around 10^5 K, to which the IPC is essentially insensitive. All the lines considered are optically thin, and hence the calculation of line intensities is straightforward (see, for example, Brown and Jordan 1981; Giampapa *et al.* 1984). In Table 1 we compare the predicted EUV line intensities to the observed line intensities (as presented by Brown and Jordan 1981) for two models which fit the obtained IPC spectra equally well, a model with low-pressure long loops and large filling factor ($f = 2.26$; model 1)³ and a model with high-pressure short loops and small filling factor ($f = 0.058$; model 2); we show the total line fluxes computed for each model (assuming the filling factor derived from our X-ray observations) in columns (2) and (3), and the observed

line fluxes (indicated in col. [4]). Because the X-ray and EUV data were not taken simultaneously, we must make the additional assumption that the transition region and corona have, on the average, not changed between the observations; the same assumption was made by Brown and Jordan (1981), who discuss in some detail the fact that, for example, line fluxes derived from low- and high-resolution *IUE* spectra, and *TD-1* and *Copernicus* line fluxes may not always be consistent. Nevertheless, we find that our results based on the X-ray observations are in accord with the *IUE* data presented by Brown and Jordan (1981).

However, we do find it impossible to simultaneously fit the *IUE*, *Copernicus*, and X-ray data, because the *Copernicus* data (an upper limit for O V, and a line detection at O VI) imply a decrease in emission measure at temperatures at $\log T \sim 5.3$ (see Fig. 2 in Brown and Jordan 1981) below the emission measure level required to explain the X-ray emission detected by the IPC. We suspect that this problem is due to either intrinsic variability, or to intercalibration difficulties (and hence is not fundamental); this point remains to be resolved. Table 1 shows that both of our loop models predict essentially the same EUV line fluxes to within the observational errors; hence neither X-ray nor EUV observations allow us to constrain the filling factor and therefore the length scales of the loops producing the observed X-ray emission. A solution to this problem appears possible only if these length scales can be directly observed (for example, by eclipses) or by use of high-resolution X-ray spectroscopy, which may allow one to distinguish between distinct coronal emission components.

IV. CONCLUSIONS

We have detected X-ray emission from the nearby system Procyon A/B (F5 V-IV + DF) with the IPC on board the *Einstein Observatory*. The fact that Procyon B is a white dwarf with relatively low surface temperature, as well as a detailed analysis of the observed IPC pulse height spectrum, including systematic errors, strongly suggests Procyon A as the source of the observed X-ray emission; this conclusion is strengthened by the fact that only one unresolved point source was detected at a position closer to Procyon A than to Procyon B. An isothermal plasma at a temperature $\log T = 6.2$ is found to satisfactorily explain the observed X-ray emission, but we reject this model on physical grounds. Modeling Procyon's corona instead with loops, all characterized by the same loop apex temperature T_{\max} and emission length scale L , we find that T_{\max} is well constrained and lies about a factor of 2 above the temperature found by assuming an isothermal plasma; however, L , and consequently the filling factor of the X-ray emitting gas, cannot be constrained, even when EUV emission from the transition region is included in the analysis.

This research was supported by NASA grants NAG8-445 and NAGW-112 and contract NAS8-30751.

³ Although model 1 apparently violates the constraint that the filling factor $f \leq 1$, we do not reject this model because the errors in, for example, the radiative cooling function can be large enough so that model 1 may in fact be consistent (with the actual $f \leq 1$). Thus, given present uncertainties in the theoretical quantities, we regard models with values of f within a factor of 2-3 of unity as consistent with a completely filled coronal atmosphere.

TABLE 1
COMPARISON OF PREDICTED EUV EMISSION WITH BROWN AND JORDAN'S OBSERVATIONS

Line (1)	Model 1 (2)	Model 2 (3)	Observed Flux (ergs s ⁻¹) (4)
C IV	8.4×10^{-12}	1.0×10^{-11}	1.2×10^{-11}
Si IV	1.6×10^{-12}	2.0×10^{-12}	1.6×10^{-12}
N V	2.1×10^{-12}	2.7×10^{-12}	1.9×10^{-12}

APPENDIX

SYSTEMATIC ERRORS IN THE ANALYSIS OF IPC SPECTRA

The two major sources of *systematic* errors are the uncertainty in the precise value of the instrument gain, which varies as a function both of time and of the position on the detector itself, and errors in the theoretically computed X-ray spectra,

used for model fitting purposes. In order to study the systematic errors thus incurred in the derived coronal parameters for Procyon A, we have fitted the observed IPC count spectrum of Procyon A assuming different instrument gains and different

TABLE 2
IPC GAIN VARIATION AND SPECTRAL MODELING

PARAMETER	PERCENT DEVIATION FROM NOMINAL DETECTOR GAIN				
	-5	-2	0	+1	+4
$\log T$	$6.32^{+0.01}_{-0.02}$	$6.27^{+0.02}_{-0.02}$	$6.24^{+0.01}_{-0.03}$	$6.21^{+0.02}_{-0.02}$	$6.14^{+0.03}_{-0.03}$
$EM/d^2 10^{50} \text{ cm}^{-3}$	0.30	0.26	0.24	0.23	0.21
χ^2	1.34	1.15	1.03	0.99	0.92

abundances; the results, i.e., temperature, emission measure (divided by square of distance) and reduced χ^2 of fit as a function of gain, are given in tabular form in Table 2 for cosmic abundances. Inspection of Table 2 shows the importance of an accurate knowledge of gain for reliable temperature determinations. We estimate that the uncertainty in instrument gain for Procyon, i.e., a point observation, is approximately 3%, hence, the uncertainty in the derived X-ray temperature is approximately 10%, strongly correlated with the adopted gain value; the error in X-ray temperature due to systematic errors in the computed emission spectra is thought to be about 0.1 in

$\log T$, and similarly, the derived emission measures are uncertain by at least 50% (J. Raymond, 1983 private communication). The derived emission measures depend strongly on temperature, and thus on gain; we therefore choose not to quote explicit errors in emission measure. Further we note that the value of the X-ray (energy) flux from Procyon is not an observed but a derived quantity, and hence depends sensitively on the assumed model (for example, isothermal plasma, loop, etc.). In conclusion, the uncertainties in the derived coronal parameters for Procyon are *strongly* dominated by systematic, and not by statistical, effects.

REFERENCES

- Allen, C. W. 1973, *Astrophysical Quantities* (London: Athlone).
 Avni, Y. 1976, *Ap. J.*, **210**, 642.
 Brown, A., and Jordan, C. 1981, *M.N.R.A.S.*, **196**, 757.
 Craig, I. J. D., McClymont, A. N., and Underwood, J. H. 1978, *Astr. Ap.*, **70**, 1.
 Cruddace, R., Bowyer, S., Malina, R., Margon, B., and Lampton, M. 1975, *Ap. J. (Letters)*, **202**, L9.
 De Loore, C., and De Jager, C. 1970, in *IAU Symposium 37, Nonsolar X- and Gamma-Ray Astronomy*, ed. L. Gratton (Dordrecht: Reidel), p. 238.
 Evans, R. G., Jordan, C., and Wilson, R. 1975, *M.N.R.A.S.*, **172**, 585.
 Giacconi, R. et al. 1979, *Ap. J.*, **230**, 540.
 Giampapa, M., Golub, L., Peres, G., Serio, S., and Vaiana, G. S. 1984, *Ap. J.*, in press.
 Golub, L., Harnden, F. R., Jr., Pallavicini, R., Rosner, R., and Vaiana, G. S. 1982, *Ap. J.*, **253**, 242.
 Gorenstein, P., Harnden, F. R., Jr., and Fabricant, D. G. 1981, *IEEE Trans.*, **NS-28**, 869.
 Hanbury Brown, R., Davies, J., Allen, L. R., and Rome, J. M. 1967, *M.N.R.A.S.*, **137**, 393.
 Hearn, A. G. 1975, *Astr. Ap.*, **40**, 355.
 Hoffleit, D. 1982, *Bright Star Catalogue* (New Haven: Yale University Press).
 Jamar, C., Macon-Hercot, P., and Praderie, F. 1976, *Astr. Ap.*, **52**, 373.
 Kahn, S. M., Wesemael, F., Liebert, J., Raymond, J. C., Steiner, J. E., and Shipman, H. L. 1984, *Ap. J.*, **278**, 255.
 Landini, M., Fossi, B. C., Paresce, F., and Stern, R. 1984, *Ap. J.*, submitted.
 Martin, C., Basri, G., Lampton, L., and Kahn, S. M. 1982, *Ap. J. (Letters)*, **261**, L81.
 Mewe, R., Heise, J., Gronenschild, E. H. B. M., Brinkman, A. C., Schrijver, J., and Den Bogende, A. J. F. 1975, *Ap. J. (Letters)*, **202**, L67.
 Morton, D. C., Spinrad, H., Bruzual, G. A., and Kurucz, R. C. 1977, *Ap. J.*, **212**, 438.
 Pallavicini, R., Peres, G., Serio, S., Vaiana, G. S., Golub, L., and Rosner, R. 1981, *Ap. J.*, **247**, 692.
 Raymond, J. C., and Smith, B. W. 1977, *Ap. J. Suppl.*, **35**, 419.
 Rosner, R., Tucker, W. H., and Vaiana, G. S. 1978, *Ap. J.*, **220**, 643.
 Serio, S., Peres, G., Vaiana, G. S., Golub, L., and Rosner, R. 1981, *Ap. J.*, **243**, 288.
 Vaiana, G. S., and Rosner, R. 1978, *Ann. Rev. Astr. Ap.*, **16**, 393.

F. R. HARNDEN, JR. and R. ROSNER: Harvard-Smithsonian Center for Astrophysics, 60 Garden Street, Cambridge, MA 02138

J. H. M. M. SCHMITT: Max-Planck-Institut für Extraterrestrische Physik, D8046 Garching bei München, West Germany

G. PERES and S. SERIO: Istituto e Osservatorio Astronomico, Palazzo dei Normanni, 90134 Palermo, Italy